International Journal of Mining Science and Technology 29 (2019) 187–198

Contents lists available at ScienceDirect

International Journal of Mining Science and Technology

journal homepage: www.elsevier.com/locate/ijmst

Determination of critical parameters in the analysis of road tunnel fires

Ali Haghighat [a,b,*], Kray Luxbacher [a]

[a] Department of Mining & Minerals Engineering, Virginia Tech, Blacksburg, VA 24061, USA
[b] Fire Life Safety, Tunnel Ventilation Group, AECOM, Oakland, CA 94612, USA

ARTICLE INFO

Article history:
Received 14 August 2017
Received in revised form 11 November 2017
Accepted 10 May 2018
Available online 12 July 2018

Keywords:
Road tunnel fire
Two-level fractional factorial design
Statistical two-level design
CFD
Fire dynamics

ABSTRACT

The analysis of the fluid characteristics downstream of a fire source in transportation tunnels is one the most important factor in the emergency response, evacuation, and the rescue service studies. Some crucial parameters can affect the fluid characteristics downstream of the fire. This research develops a statistical analysis on the computational fluid dynamics (CFD) data of the road tunnel fire simulations in order to quantify the significance of tunnel dimensions, inlet air velocity, heat release rate, and the physical fire size (fire perimeter) on the fluid characteristics downstream of the fire source. The selected characteristics of the fluid (response variables) were the average temperature, the average density, the average viscosity, and the average velocity. The prediction of the designed statistical models was assessed; then the significant parameters' effects and the parameters interactive effects on different response variables were determined individually. Next, the effect of computational domain length on the selection of the significant parameters downstream of the fire source was analyzed. In this statistical analysis, the linear models were found to provide the statistically good prediction. The effect of the fire perimeter and the parameters interactive effects on the selected response variables downstream of the fire, were found to be insignificant.

1. Introduction

In order to provide the fire safety plan of the occupants and the emergency response layout in the road tunnel fire situations, there is a crucial need to understand the factors that may influence the conditions of people exposed to the closed space (e.g., transportation tunnel) fires. Due to the interaction of physical and chemical processes (turbulence, combustion, radiation, etc.) in a closed space, tunnel fires are complex phenomena [1]. As a result, fire life safety in a tunnel must be carefully considered. Tunnel safety ties to the tunnel design, the tunnel management, and the emergency response. The dimensions of the tunnel (width, height, and length) which are the main parameters of the tunnel design, can play a key role in changes of the build-up heat rate and the rate of smoke stratification during the fire events. The other important parameter of the tunnel design, which affects the tunnel safety, is the ventilation system. The airflow velocity can influence the smoke propagation upstream and downstream of the fire in road tunnel fire events. The second most important element in assessing the tunnel safety, is the traffic management in transportation tunnels. A thorough understanding of the nature of the transportation vehicles (e.g., the size of the vehicles, the produced heat release rate (HRR) output from the fire during a fire event) commuting through a tunnel, can help to design safer, and more reliable emergency response layout [2].

Previous studies have shown that the smoke generation and fire behavior are affected by different parameters such as HRR, ventilation, the dimensions of the obstruction, [3–6]. Babrauskas and Peacock indicated that HRR is the single most important variable in fire hazard analysis [3]. The other important parameter in terms of smoke propagation is ventilation. Since tunnel fires have limited air access points [4], the fire was assumed to be a fuel-controlled fire in this research study. Therefore, the tunnel dimension, the air velocity, the physical fire size, and the HRR are the most important parameters affecting the transportation tunnel safety.

There is an experimental study on the effect of tunnel cross section and the velocity together on gas temperatures and heat fluxes for the large HRR fire sources (HRR $\geq$ 100 MW). In that study, it was proven that the maximum temperature under the ceiling was significantly dependent on the tunnel height changes, while the tunnel width changes, HRR changes, and the longitudinal velocity changes had insignificant impacts on the maximum temperature under the ceiling. In addition, that study showed that by increasing the tunnel dimensions, the downstream temperature

* Corresponding author at: Department of Mining & Minerals Engineering, Virginia Tech, Blacksburg, VA 24061, USA.
E-mail address: ali.haghighat@aecom.com (A. Haghighat).

https://doi.org/10.1016/j.ijmst.2018.05.003
2095-2686/© 2018 Published by Elsevier B.V. on behalf of China University of Mining & Technology.

decreased [5]. And also, some studies were carried out to determine and calculate the HRR of the vehicle fires in the road tunnels experimentally and numerically [7,8] which the results can be utilized to the design more reliable emergency response layout. Therefore, the transport of the smoke and the transfer of the heat were affected by the explained parameters. Based on previous research studies, the smoke, heat, and fire products impacted the physical abilities of the occupants [9–12] which they can have an immense impact on the design of the evacuation plans. Although the impact of explained parameters on the physical abilities of the occupants were investigated, the interactive effect of different parameters (e.g., tunnel dimension, inlet velocity, HRR, and the fire perimeter) were not investigated. Also, the research studies on determination of the significant parameters on changes of the temperature, density, velocity, and viscosity downstream of the fire source in transportation tunnels are so limited. In addition, the effect of computational domain length on the selection of the significant parameters for changes of the fluid characteristics (e.g., average temperature, average density, average viscosity, and average velocity) downstream of the fire source was not quantified in previous studies.

The focus of the research in this paper is to utilize a two-level statistical approach to investigate the effect of the tunnel dimensions, the inlet air velocity, HRR, the fire perimeter, and the parameters interactive effect on the fluid characteristics at different cross sections downstream of the fire. Eight different CFD vehicle fire scenarios for the road tunnel were simulated in fire dynamics simulator (FDS), Version 6.0 which we refer the reader to the FDS technical reference guide [13] for the detailed numerical algorithm in this software. Then, the fluid characteristics such as average temperature, average density, average velocity, and average viscosity at different tunnel cross sections were calculated. The calculated CFD results were analyzed in order to conduct a statistical analysis (a two level fractional factorial design) for determination of the significant parameters on the mentioned fluid characteristics downstream of the fire source. The linear, quadratic and cubic statistical models were investigated and the prediction of the designed statistical models were assessed via residual analysis and the studentized residuals versus predicted values analysis. Next, the significant parameters on the fluid characteristics at a selected cross section downstream of the fire was determined based on the performed two-level fractional factorial design. Moreover, the effect of the domain length on the significant parameters determination downstream of the fire source was analyzed. The outcomes of this research can be utilized to decrease the number of simulations in future studies by determination of the significant and insignificant parameters on the change of the fluid characteristics downstream of the fire source. In addition, the findings of this study can be used to modify the tunnel design, the tunnel management (e.g., operational management, traffic management, and the engineering management), firefighting procedures, and the emergency medical assistance, and more robust emergency response layout.

2. Parametric study and design considerations

A two-level statistically designed program was conducted to quantify the significant parameters on the responses at different cross sections, downstream of the fire. The two-level fractional factorial design has different advantages. One of the most important its advantages is that the interaction of different parameters on a specified response can be investigated. In addition, fewer experiments can be conducted with the use of fractional factorial deign compare to the full factorial design. Furthermore, with the usage of factorial design, the error variance can be decreased [14]. This approach is common to be used to screen the significant parameters on various responses in different research areas [15,16]. For the initial screening stage of a research study, the fractional factorial designs were recommended as the good alternatives to the full factorial designs [17]. Although the full factorial designs (e.g., 16 simulations in this study) were the desirable designs, the two-level fractional factorial design (e.g., 8 simulations) was considered for screening of the significant parameters on the selected response variables. The resolution of the selected two-level fractional factorial design in this study was IV which is one where no significant effect is confounded with any other significant effect or 2-factor interaction [17,18]. In addition, the resolution IV is common to be utilized for application of fractional factorial design in research studies [18].

A two-level test program based on the fractional factorial design was performed to evaluate the effects of the heat release rate (HRR), physical fire size, tunnel cross section, and the inlet velocity on the responses such as the average temperature, the average density, the average velocity, and the average viscosity at the cross sections downstream of the fire. Therefore, four main parameters as shown in Table 1 were selected due to the previous research studies results. A minimum and a maximum values were selected for each parameter. In this study, the regular van and bus sizes were used as the minimum and maximum physical fire sizes respectively in this study. Although in NFPA® 502, 2011, it is recommended that 30 MW and 10 MW be used as the peak heat release rates for the bus and the van respectively [19], for investigation of the effect of fire perimeter on different response variables, 30 MW and 10 MW were also considered for the van and the bus fire heat release rate respectively. The width, length, and the height of the van and bus used in the computational domain were $1.7 \times 5.0 \times 2.4$ m^3 and $2.7 \times 12.0 \times 3.5$ m^3, respectively. Two and three lane standard cross section of road tunnels [20] were considered in this study. The height of the tunnel was set to 7.7 m as the height of Gotthard tunnel in Switzerland. Although pedestrians are not permitted in road tunnels, sidewalks are required and recommended to be greater than or equal to 0.7 m [21]. Therefore, two 0.96 m sidewalks were considered in the geometry of the road tunnels. The length and the height of the whole tunnels were 960 m, and 7.7 m, respectively. The width of the tunnel for the two and three lane transportation tunnels were set to 9.6 m and 15.6 m respectively. The detailed tunnel geometry dimensions used in the simulations are shown in Fig. 1a and b.

The selection of the fluid characteristics (e.g., the average temperature, average density, average velocity, and average viscosity) are based on the needs for providing necessary information for fire brigade teams and firefighters to develop more effective firefighting operations. The gas temperature and the airflow velocity can affect the access to the tunnel [22]. Therefore, the average temperature and the average velocity were selected as two key response variables in this study. The concentration of combustion products (toxic species (e.g., CO, CO_2)) was not considered in this research study since the fire brigade and firefighters carry self-contained breathing apparatus (SCBA) in the operations [19]. Since the viscosity of the fluid is temperature dependent and can affect the heat transfer [23], the average viscosity was selected as the parameter of interest in this study. In addition, the average density was selected as one of the fluid characteristics in this research study since it affects the local visibility.

All of the studies on roll back and critical velocity showed that for the 10 MW to 100 MW fires, the critical velocity varies from 2.5 m/s to 3 m/s [24–28]. It should be considered that the critical velocity can vary due to different hydraulic diameters. Therefore, a study was conducted to calculate the critical velocity for 10 MW and 30 MW vehicle fires in both two and three lane road tunnels with the following equations:

Table 1
Two levels (a minimum and a maximum).

Parameters	Minimum	Maximum
Heat release rate (MW)	10	30
Physical fire size (m^3)	Van size (20.4)	Bus size (113.4)
Tunnel cross section (m^2)	73.7 (2 lane)	119.8 (3 lane)
Inlet air velocity (m/s)	1.5	5.0

$$V_c = K_1 K_g \left[\frac{gHQ}{\rho C_p A T_f}\right]^{1/3} \tag{1}$$

$$T_f = \left[\frac{Q}{\rho C_p A V_c}\right] + T \tag{2}$$

where V_c is the critical velocity, m/s; K_1 the Froude number factor; K_g the grade factor; g the acceleration caused by gravity, m/s^2; H the height of duct or tunnel at the fire site, m; Q the heat fire is adding directly to air at the fire site, kW; ρ the average density of the approach (upstream) air, kg/m^3; C_p the specific heat of air, kJ/(kg·K); A the area perpendicular to the flow, m^2; T_f the average temperature of the fire site gases, K; and T the temperature of the approach air, K [19]. The calculated hydraulic diameters for both two lane and three lane road tunnels were 8.53 m and 10.30 m, respectively. The critical velocity varied from 2.6 m/s to 3.7 m/s for 10 MW and 30 MW fires in the associated tunnels. Since the inlet velocity affects the propagation of the smoke and hot gases to the upstream and the downstream of the fire source, a velocity less than critical velocity (1.5 m/s < V_{cr}) and a velocity greater than critical velocity (5 m/s > V_{cr}) were selected for investigation of significant parameters on different responses (e.g., mean temperature, mean velocity, mean viscosity, and mean density) at different cross sections downstream of the fire.

The *t*-squared approach was utilized for the growth of the vehicle fires [29]. Based on previous study, the time to reach maximum HRR (t_{max}) for van fire and bus fire were recommended to be 5 min and 10 min, respectively [29]. However, because of the simulation cost, 1 min was considered as the t_{max} in all simulations. Since the focus of this research study is to investigate the effect of some parameters on the response variables changes during a fire event, the decay time period for vehicle fires was not considered. Flexible polyurethane foam characteristics as shown in Table 2 were used for vehicle fire simulation in the tunnels [30].

The thermal and the physical characteristics of the concrete such as density, thermal conductivity, and specific heat were considered for the characteristics of the tunnel's side walls, roof, and the sidewalks [31]. The thermal diffusivity of concrete was set to 0.77 mm^2/s [32]. All the thermal characteristics of the concrete was based on the rock type in the concrete which was assumed to be limestone, sandstone, and chert. And also the sand and aggregate were from the same rock type at early age. The thermal and the physical characteristics of the asphalt were considered for the characteristics of the tunnel pavement. The density, thermal conductivity, and specific heat capacity of the dry asphalt with 5% air voids content were set to 2371.67 kg/m^3, 1.16 W/m °C, and 0.9637 kJ/kg °C, respectively [33]. The ambient air temperature, ambient air density, and air viscosity at ambient temperature were set at 20 °C, 1.196 kg/m^3, and 1.79×10^{-5} kg/(m·s) respectively in all simulations. Although in FDS the "log law" wall model is employed for the rough walls [13], the no-slip boundary condition still can be utilized if it is needed. Since the smooth concrete was considered for the road tunnels' walls in this study, the "log law" wall model was overridden and the no-slip boundary condition was set for all walls, sidewalks, roof, pavement, and the objects in the domain. For the detailed "log law" wall model explanation, we refer the reader to the FDS technical reference guide [13]. Fixed air flows based on two different velocities were set to the inlet of computational domain since the jet fans were assumed to be far away from the fire source. Reliable numerical results can be achieved when the grid size is $\leq 0.1D*$ [34], where $D*$ is explained in detail in [35,36]. Therefore, the rectangular cells with a grid size of 24 cm was considered for the numerical analysis based on the used heat release rates (10 MW and 30 MW) in this research study. The turbulent viscosity in all simulations was considered as the Deardorff [37,38] turbulent viscosity with 0.1 as the Deardorff coefficient (C_v). The turbulent diffusivity was obtained using a 0.5 as the constant Schmidt number (Sc_t) (for mass diffusivity) and a 0.5 as the constant Prandtl number (Pr_t) (for thermal diffusivity). The default value (0.35) was considered as the radiative fraction (the fraction of energy released from the fire as thermal radiation) in this study. The mixing-controlled combustion [13] was considered as the combustion model in this study since the finite-rate combustion model was not computationally efficient [39] for large-scale fire scenarios.

Table 2
Heat of combustion, CO, CO_2, and soot yields of vehicle fire events in simulation.

Material	ΔH_T (kJ/kg)	Y_{CO2} (kg/kg)	Y_{CO} (kg/kg)	Y_{Soot} (kg/kg)
Polyurethane	25,300	1.5325	0.02775	0.1875

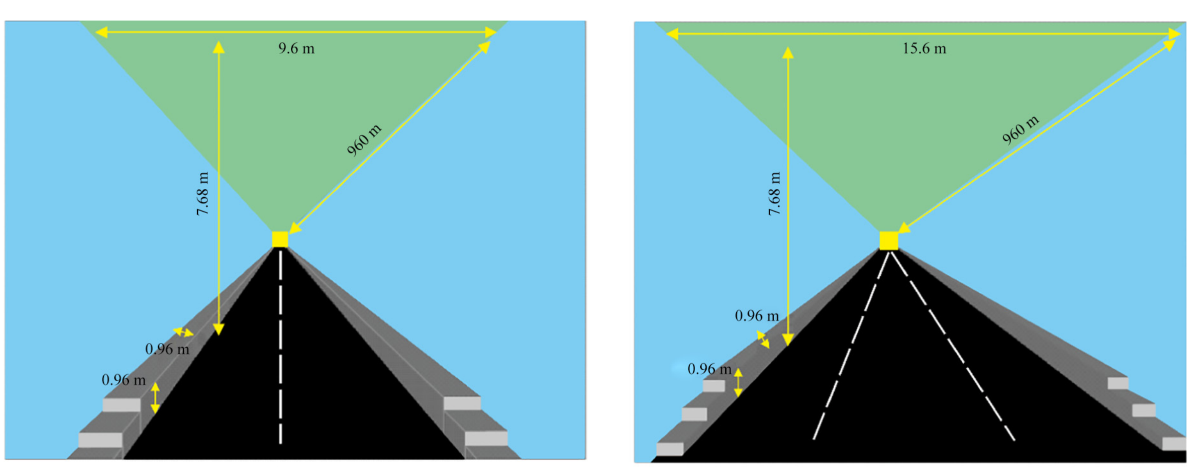

(a) Two lane (b) Three lane

Fig. 1. Transportation tunnel detailed dimensions.

Table 3
CFD simulation scenarios based on different parameters.

Scenarios	Parameter 1 Inlet air velocity (m/s)	Parameter 2 HRR (MW)	Parameter 3 Fire size (m^3)	Parameter 4 Tunnel dimension (m^2)
Scenario 1	5.0	10	Bus (114.0)	2 lanes (73.7)
Scenario 2	5.0	30	Van (20.3)	2 lanes (73.7)
Scenario 3	1.5	10	Van (20.3)	2 lanes (73.7)
Scenario 4	1.5	30	Bus (114.0)	2 lanes (73.7)
Scenario 5	1.5	10	Bus (114.0)	3 lanes (119.8)
Scenario 6	5.0	30	Bus (114.0)	3 lanes (119.8)
Scenario 7	5.0	10	Van (20.3)	3 lanes (119.8)
Scenario 8	1.5	30	Van (20.3)	3 lanes (119.8)

Consequently, eight computational fluid dynamics (CFD) scenarios as shown in Table 3 were simulated to investigate the effect of mentioned parameters (Table 1) on average temperature, average density, average velocity, and viscosity at different cross sections downstream of the fire. All the vehicle fires were set at the middle of the road tunnels.

3. CFD results and discussion

To conduct the statistical assessment for determination of the significant parameters (e.g., HRR, physical size of the fire (fire perimeter), tunnel dimension, and airflow velocity) on the fluid characteristics downstream of the fire, there was a need to calculate the average temperature, viscosity, density, and velocity along the height of the tunnel at different cross sections in all scenarios. All parameters were calculated every 5 m upwind and downwind from the fire source and the zero line is the representative of the tunnel cross section at the center of the fire source as shown in Fig. 2.

The calculated results for average temperature, average density, average viscosity, and average velocity along the height of the tunnel at different cross sections for all scenarios are shown in Figs. 3 and 4. It is noteworthy that the rollback did not advance significantly along the X axis after 900 s and the steady-state flow condition in the tunnel was reached at $t = 900$ s in all scenarios. Therefore, all parameters upwind and downwind of the fire source were calculated at $t = 900$ s in all scenarios. Due to the considered inlet velocity less than the critical velocity in some scenarios (e.g., scenarios 3, 4, 5, and 8), the upwind transport of the smoke (backlayering phenomenon) was observed. The length of the backlayering (rollback) for scenarios 3, 4, 5, and 8 was calculated at 170 m, 270 m, 150 m, and 273 m respectively from the centerline of the fire source. In the rest of the scenarios (e.g., scenarios 1, 2, 6, and 7), due to the velocity greater than critical velocity, just the downwind transport of the smoke was observed.

Since, just the downwind transport of the smoke was observed in scenarios with the velocity greater than critical velocity (e.g., scenario 1, 2, 6, and 7), the average temperature, average density, average viscosity, and the average velocity upstream of the fire source was calculated similar to the ambient ones as can be seen in Figs. 3 and 4. According to Fig. 3a, by getting further from the fire source, the average temperature along the height of the tunnel at different cross sections decreased, as expected. The decreasing temperature trend downstream of the fire continued until it eventually ends up the ambient temperature (20 °C). Consistent with the data of Fig. 3a, it is evident that the average temperature was 20 °C in scenarios with the velocity greater than critical velocity (scenarios 1, 2, 6, and 7) from the inlet to 4 m from upwind of the end of the fire object, while because of the upwind transport of the smoke (rollback) in scenarios with velocity less than critical velocity (e.g., scenarios 3, 4, 5, and 8), the average temperature at different cross sections upstream of the fire varied. The highest mean temperature at the fire source was calculated in scenario 4 (373 °C), due to the highest HRR, the lowest velocity, and the smallest tunnel cross section among all scenarios. Due to the dependency of the density to the temperature, the lowest average density at the fire source was calculated in scenario 4 as shown in Fig. 3b. According to Fig. 3b, it is noteworthy that no appreciable variations in average air density could be observed downstream of the fire source, when the CFD domain length is larger than 300 m. The average density upstream of the fire source was influenced by the upstream transport of smoke and hot gases (backlayering) in scenarios with velocity less than critical velocity

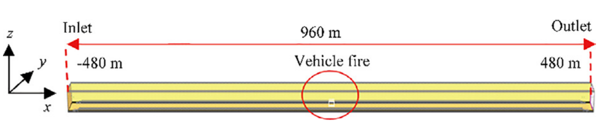

Fig. 2. The isometric view of the computational domain.

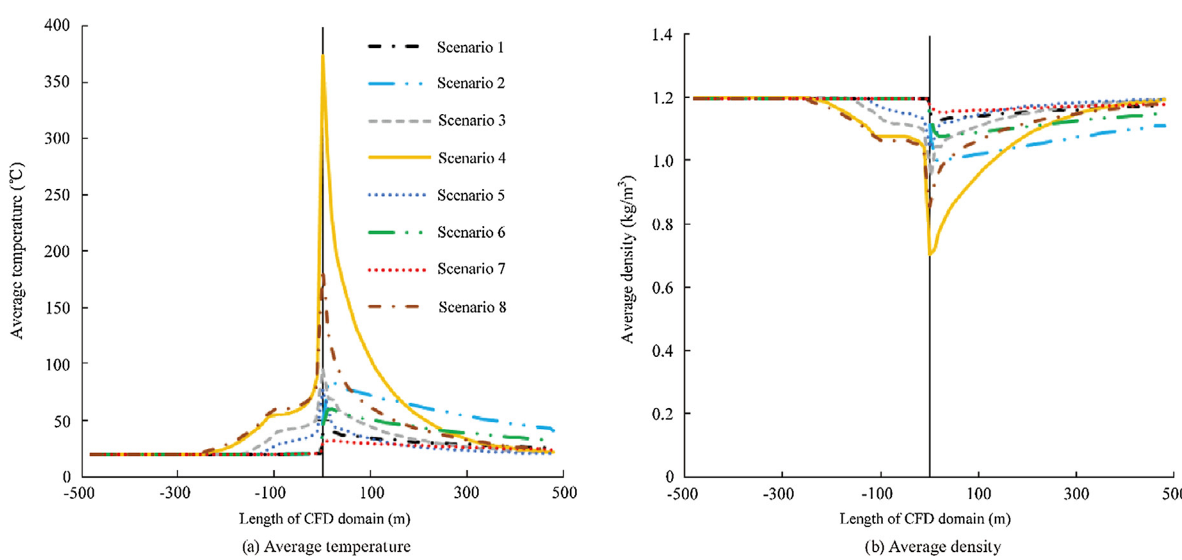

Fig. 3. Fluid characteristics along the height of the tunnel at different cross sections of the road tunnel at $t = 900$ s for all scenarios (0 on the X-axis represents the middle plane of fire source).

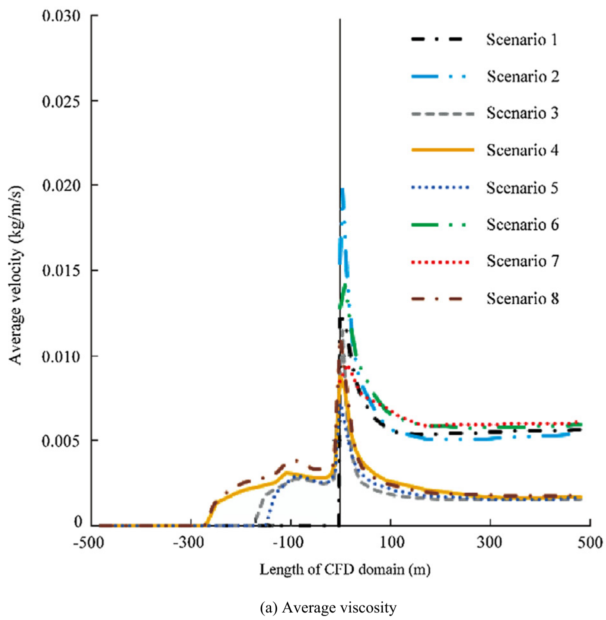

Fig. 4. Fluid characteristics along the height of the tunnel at different cross sections of the road tunnel at $t = 900$ s for all scenarios (0 on the X-axis represents the middle plane of fire source).

(scenarios 3, 4, 5, and 8). However, the average density was measured as same as the inlet air density from the inlet to 4 m from upwind the end of the fire object in scenarios that the velocity was greater than the critical velocity (e.g., scenarios 1, 2, 6, and 7) as shown in Fig. 3b.

The average viscosity and average velocity along the height of the tunnel at different cross sections were calculated as shown in Fig. 4a and b respectively. According to Fig. 4a, there were no appreciable variations observed downstream of the fire source, when the CFD domain length is larger than 100 m in all scenarios. Furthermore, the average viscosity and average velocity were measured as 1.79×10^{-5} kg/m/s and 5 m/s, respectively, for scenarios with the velocity greater than critical velocity (scenarios 1, 2, 6, and 7) from the inlet to 4 m from upwind the end of the fire source. The rollback influenced on the average viscosity and the average velocity at different cross sections upstream of the fire source in scenarios with the velocity less than critical velocity (e.g. scenarios 3, 4, 5, and 8) as shown in Fig. 4a and b. Because of the highest HRR, highest velocity, and the smallest cross section in scenario 2 compared to the other scenarios, the highest viscosity was calculated at 3.5 m downstream of the fire source.

4. Parametric evaluation

A statistically-designed parametric study was performed to investigate the influence of independent variables (e.g., the tunnel dimension, the physical fire size, HRR, and the velocity) on the dependent responses (e.g., the mean temperature, the mean density, the mean velocity, and the mean viscosity) downstream of the fire source, statistically. Four different cross sections, shown in Table 4, downstream of the fire were considered to conduct the statistical analysis for determination of the significant parameters on temperature, velocity, viscosity, and density changes. Cross sections 1 to 4 were classified based on a distance from the centerline of the fire source.

To evaluate the parameters and the parameters interactive effects, eight CFD simulations were developed as described in the sections 2 and 3. The repetitive simulations were ignored in this statistical analysis since the similar results were calculated. Next,

Table 4
Selected cross sections for calculation of the average variable responses.

Cross section	Downstream distance (m)
Cross section 1	20
Cross section 2	120
Cross section 3	220
Cross section 4	400

the response variables (e.g., average temperature, average density, average velocity, and average viscosity) along the height of the tunnel at four selected cross sections (cross sections 1, 2, 3, and 4) at $t = 900$ s were calculated. The calculated values for the response variables 120 m downstream of the fire source (cross section 2) are provided in Table 5 (see Appendix A for the response variables at the cross sections 1, 3, and 4). The selection of cross section 2 was based on previous studies that the location to couple CFD models to 1D models downstream of the fire should be at least 12 times the hydraulic diameter [40].

The accuracy of the prediction of the statistical model is related to the selected statistical model [41,42]. In this statistical analysis, the linear, quadratic and cubic models were investigated. A residual analysis was conducted to make sure the statistical models are well-behaved. The normality of residuals were assessed via the normal probability plot of the studentized residuals as shown in Fig. 5a–d for all models which indicates that the error terms were normally distributed when the linear model was performed.

Additionally, the studentized residuals versus predicted values were investigated for three main reasons. First, they were utilized to check that the residuals bounce randomly around the 0 line which indicates that the assumption that the relationship is linear is reasonable. Second, they were used to check the residuals roughly form a horizontal band around the 0 line which indicates that the variances of the error terms are equal. Third, they were used to check that there are no outliers if no one residual stands out from the basic random pattern of residuals [43]. Consistent with the data from the studentized residuals versus predicted values plots, it was evident that there were no unusual data points in

Table 5
Summary of independent parameters and measured average values for the response variable at cross section 2 (120 m downstream of the fire source) at $t = 900$ s.

Scenario No.	Response variables			
	Temperature (°C)	Density (kg/m^3)	Velocity (m/s)	Viscosity (kg/m/s)
Scenario 5	30.69	1.16	1.65	0.00196
Scenario 8	52.77	1.09	1.88	0.00218
Scenario 2	70.60	1.02	5.99	0.00551
Scenario 1	33.93	1.14	5.34	0.00556
Scenario 3	42.14	1.12	1.75	0.00179
Scenario 4	96.59	0.97	2.05	0.00254
Scenario 7	28.78	1.16	5.32	0.00623
Scenario 6	48.42	1.10	5.64	0.00620

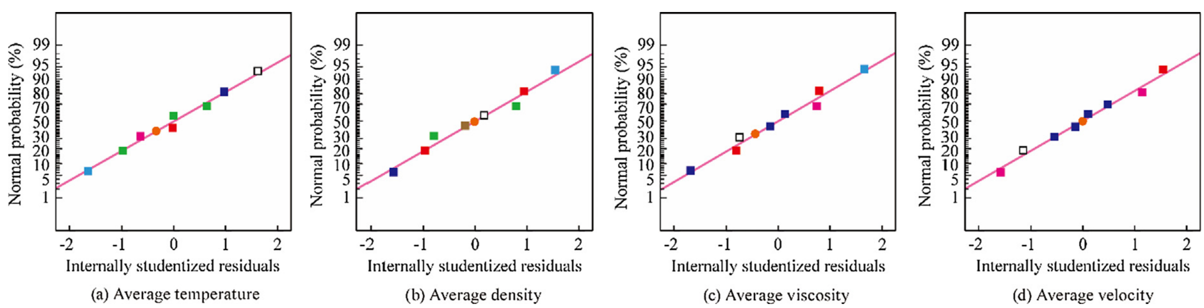

Fig. 5. Normal plot of residuals, at cross section 2 (120 m downstream of the fire) for eight scenarios at $t = 900$ s for different variable responses.

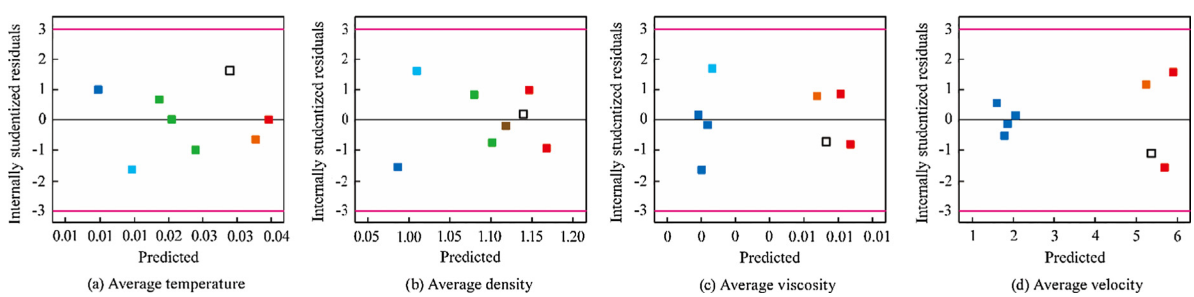

Fig. 6. Residuals versus predicted plots, at cross section 2 (120 m downstream of the fire) for eight scenarios at $t = 900$ s for different variable responses.

the data set. In addition, the results have shown that the variation around the estimated regression line is constant, suggesting that the assumption of equal error variances was reasonable as plotted in Fig. 6a–d for average temperature, average density, average viscosity, and average velocity at cross section 2 (120 m downstream of the fire source).

The same studies were conducted at the other cross sections (cross section 1, cross section 3, and cross section 4) in order to investigate the behavior of statistical models when the cross sections were changed. The same behavior was observed when the linear model was utilized at the other cross sections. All in all, the linear models were found to provide statistically good prediction at four selected cross sections downstream of the fire source. The p-values obtained from ANOVA for linear models were calculated less than 0.05 for all models which indicates the models are significant as shown in Table 6 (see Appendix B for the probability of the significant parameters or significant associated interactions on various responses at the cross sections 1, 3, and 4).

Moreover, the coefficient of determination (R^2) was utilized to show that the estimated response variables were accurate by the usage of the models. The R^2 greater than 0.9 indicated that the linear models could predict the average temperature, average viscosity, average velocity, and average density at determined interface boundary accurately. The adjusted coefficient of determination ($R^2_{adj.}$) was quantified for each data set to show that each model was not constrained by a low degree of freedom. The difference between the coefficient of determination and the adjusted coefficient of determination was measured less than 0.0276 at cross section 2 (120 m downstream of the fire) for all of the models as shown in Table 6. Therefore, the required standard was met. After acceptance of the model, the parametric and parameter interaction terms were evaluated to determine the significant terms statistically. The null hypothesis for the assessment was that the corresponding coefficient value was zero. The probability of the significant parameters or significant associated interactions on various responses at cross section 2 (120 m downstream of the fire) are shown in Table 6 (see Appendix B for the probability of the significant parameters or significant associated interactions on various responses at the other cross sections). The criterion for the rejection of insignificant terms was set to a t-value greater than 0.05 confidence level. The t-values for significant parameters are shown in Table 6. The inlet air velocity, HRR, the physical fire size (fire perimeter), and the tunnel dimension are characterized by *A*, *B*, *C*, and *D* respectively. Therefore, the interaction of two parameters could be distinguished via using two letters (e.g., *AD* is the interaction of their velocity and the tunnel dimension).

The primary parameters affecting the average temperature at cross section 2 (120 m downstream of the fire) were, in order of

Table 6
Statistical significance of the parameters and their associated interactions along with fit analysis for the models at cross section 2 (120 m downstream of the fire).

Average temperature		Average viscosity		Average velocity		Average density	
Parameter	T-Statistic	Parameter	T-Statistic	Parameter	T-Statistic	Parameter	T-Statistic
Model	0.0002	Model	0.0011	Model	<0.0001	Model	0.0073
B-HRR	<0.0001	A-Inlet air velocity	0.0002	A-Inlet air velocity	<0.0001	B-HRR	0.0024
D-Tunnel dimension	0.0008			B-HRR	0.0132	D-Tunnel dimension	0.0098
R-Squared	0.9904	R-Squared	0.9944	R-Squared	0.9989	R-Squared	0.9794
Adj. R-Squared	0.9831	Adj. R-Squared	0.9869	Adj. R-Squared	0.9975	Adj. R-Squared	0.9518

significance, the HRR, the tunnel dimension, the inlet air velocity, and the interaction of the inlet air velocity and the tunnel dimension. According to the *p*-value results in Table 6, the HRR and the tunnel dimension had significant contributions on the average temperature changes compare to the other parameter effects on the average temperature (the insignificant parameters (e.g., the inlet air velocity (*A*) and the interaction of the inlet air velocity and tunnel dimension (*AD*)) were excluded from the Table 6). The effect of HRR and the tunnel dimension on the average temperature changes at cross section 2 (120 m downstream of the fire) are shown in Figs. 7 and 8 respectively. By varying the HRR from 10 MW to 30 MW, the average temperature at cross section 2 (120 m downstream of the fire) increased conspicuously as shown in Fig. 7. The temperature increased from 42.1 °C to 96.6 °C when the HRR changed from 10 MW to 30 MW in the two lane tunnel with a 1.5 m/s inlet air velocity.

The other significant parameter on the changes of the average temperature at cross section 2 was the tunnel cross section as shown in Fig. 8. According to Fig. 8, by increasing the tunnel dimension from 2 lane (9.6 m width) to 3 lane (15.6 m width), the average temperature at cross section 2 (120 m downstream of the fire) significantly decreased from 100 °C to 50 °C when the HRR and the velocity were 30 MW and 1.5 m/s respectively. In addition, it was observed that by changing the velocity from 1.5 m/s to 5 m/s, for 10 MW and 30 MW fire scenarios at cross section 2 (120 m downstream of the fire), the average temperature did not experience a drastic change except for the 30 MW fire in a two lane road tunnel as shown in Fig. 8a. All in all, the average temperature in the two lane tunnel was calculated higher compared to the average temperature in the three lane road tunnel a cross section 2. It is noteworthy that changes to the physical size of the fire (fire perimeter) did not affect the average temperature at cross section

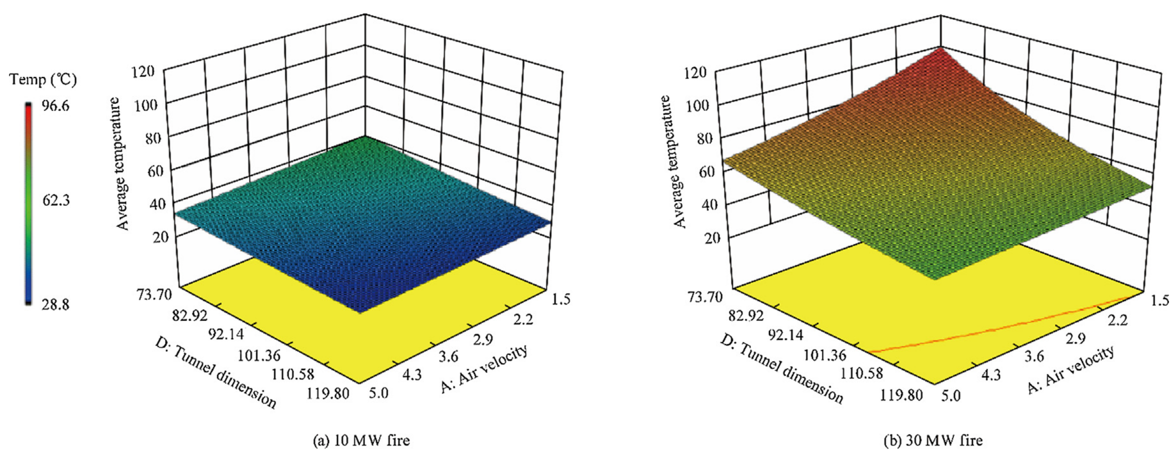

Fig. 7. Effect of the HRR on the average temperature at cross section 2 (120 m downstream of the fire) at $t = 900$ s: 10 MW fire and 30 MW fire.

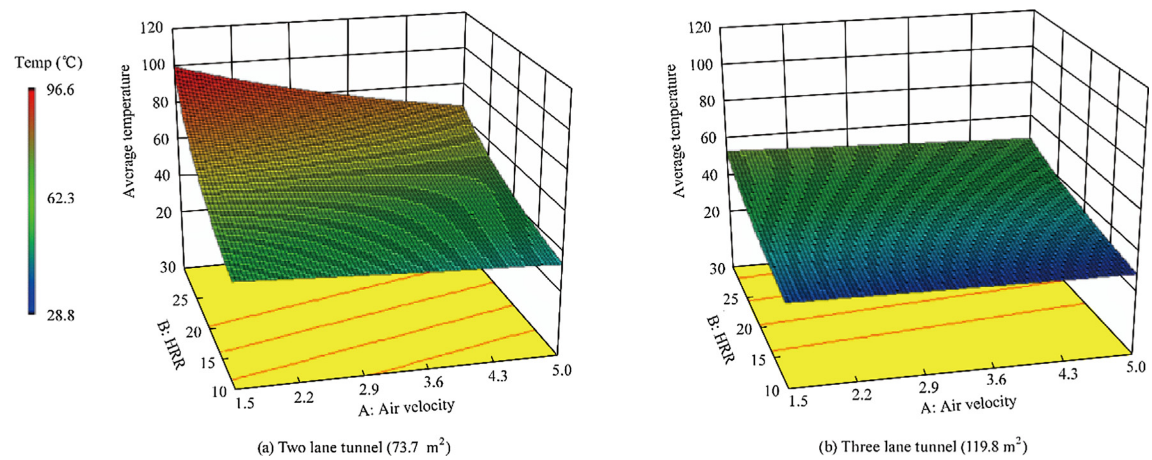

Fig. 8. Effect of the tunnel dimension on the average temperature at cross section 2 (120 m downstream of the fire) at $t = 900$ s: two lane tunnel (73.7 m^2) and three lane tunnel (119.8 m^2).

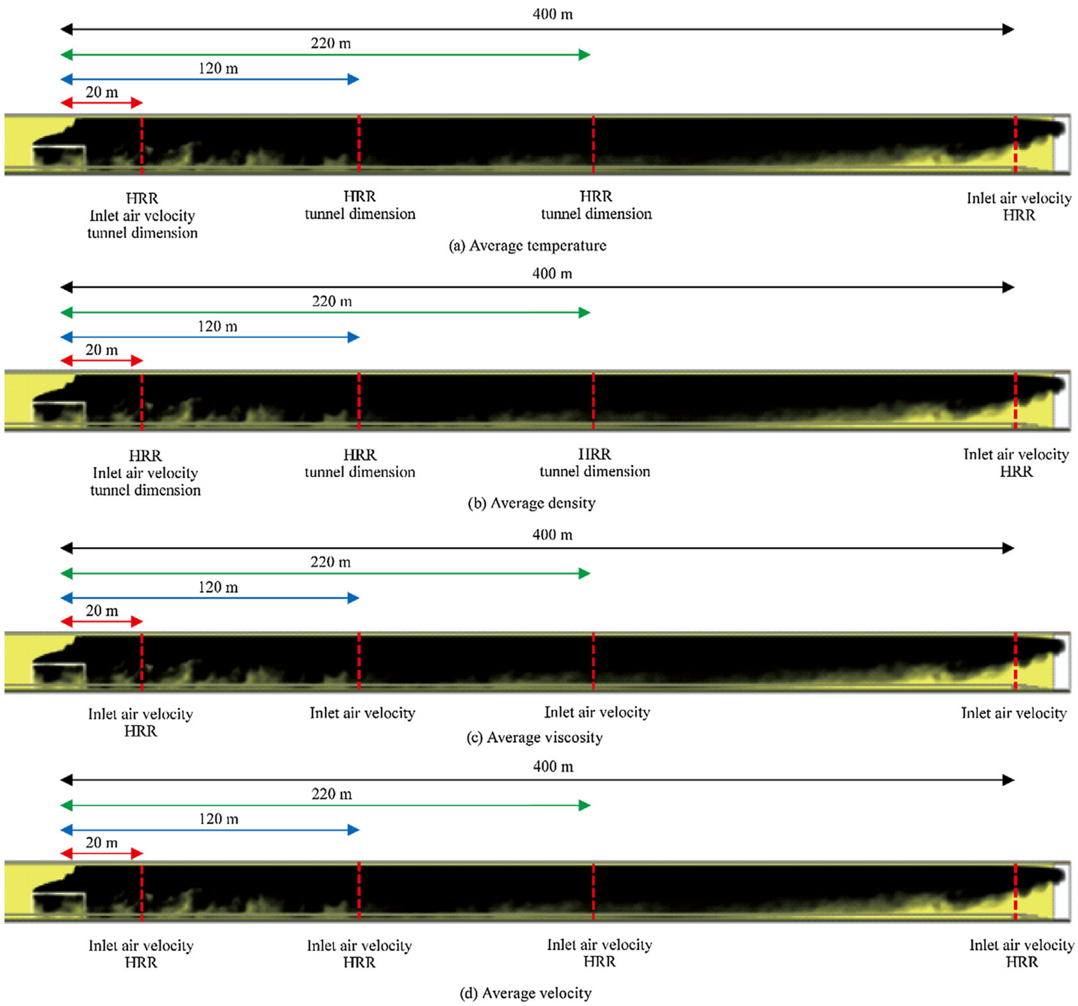

Fig. 9. Significant parameters on different response variables at different cross sections downstream of the fire source.

2 (120 m downstream of the fire). And also, the interactive effect of other parameters were observed insignificant on the average temperature changes, 120 m downstream of the fire source.

The inlet air velocity was determined as the only significant parameter on the average viscosity changes at cross section 2 as shown in Table 6. This study indicates that the other parameter effects or parameter interactions effects on the average viscosity changes were inconsequential (e.g., the effect of HRR changes, tunnel dimension changes, the physical fire size changes), and their interaction on the average viscosity were inconsequential. According to Table 6, the significant parameters on the average velocity changes 120 m downstream of the fire source, in order of significance, were the inlet air velocity and the HRR. Therefore, it was observed that the mean velocity at cross section 2 (120 m downstream of the fire) was changed dramatically, by changing the inlet air velocity and the HRR. Due to the dependency of density to the temperature, the significant parameters on average temperature and average density changes were observed the same (e.g., significant parameters were HRR and tunnel dimension) at cross section 2 (120 m downstream of the fire) as shown in Table 6.

5. Effect of domain length on significant parameters determination

Due to complex dynamical fluid field close to the fire source, different parameters such as temperature, velocity, viscosity, and density close to the fire source could behave differently compare to the values far away from the fire source. Therefore, the significant parameters (e.g., tunnel dimension, physical fire size, HRR, and inlet air velocity) on the changes of the response variables could be different close to the fire source compare to the far away from the fire. Due to this, three different cross sections (cross section 1, cross section 3, and cross section 4) were selected to conduct a statistical analysis for determination of the significant parameters on different response variables at the selected cross sections downstream of the fire. Based on the calculated response variables at selected cross sections downstream of the fire (see Appendix A), the ANOVA test for linear models as shown in Appendix B were conducted and the significance of the models were assessed based on the *p*-values. The calculated *p*-values obtained from ANOVA for the linear models were less than 0.05 for all models which indicates that the models were significant as shown in Appendix B. Then, the significant parameters on the selected response variables were determined at different cross sections downstream of the fire as shown in Fig. 9. The colors in Fig. 9 associated with the distance from the fire source.

Consistent with the data of Appendix B and Fig. 9a, it was observed that by getting further from the fire source, the significance of the tunnel dimension on the average temperature at the cross sections decreased from the cross section 1 to the cross section 4. The effect of tunnel dimension on the average temperature changes was insignificant 400 m downstream of the fire source (cross section 4). It is noteworthy that the inlet air velocity was the significant parameter on average temperature changes at cross section 1 (20 m downstream of the fire source) and the cross section 4 (400 m downstream of the fire source) as shown in Fig. 9a. However, it was an insignificant parameter on average temperature changes at the cross sections 2 and 3 (120 m and 220 m downstream of the fire source). The reason lies in the decreasing trend of the average temperature in the simulations with velocity greater than critical velocity ($V \geq V_{cr}$) compare to the results of the scenarios with velocity less than critical velocity ($V < V_{cr}$) as shown in Fig. 10. By getting further away from the fire source, the average temperature downstream of the fire source decreased faster in the scenarios that have the inlet air velocity less than critical velocity $V < V_{cr}$ (1.5 m/s) in comparison with the scenarios that have the inlet air velocity greater than equal to the critical velocity $V \geq V_{cr}$ (5 m/s). According to Fig. 10, the average temperature difference at the center of the fire source ($X = 0$) was consequential for the same two scenarios with different velocities (e.g., scenarios 1 vs 3, 2 vs 4, 5 vs 7, and 6 vs 8). However, when you get further from the fire source, the average temperature difference decreased until the average temperature was equal at a given cross section as shown in Fig. 10 (red points). The average temperature difference between two scenarios with the same HRR and tunnel dimensions, but different inlet air velocities at that point (red points), was calculated as zero. Therefore, the effect of the inlet air velocity on the average temperature changes at that point was inconsequential. And after that, the average temperature difference again increased, so, the effect of the inlet air velocity on the average temperature increased. In addition, it was observed that the HRR was the only significant parameter on the changes of the temperature at all cross sections downstream of the fire source as shown in Fig. 9a.

Since the density is temperature dependent, the significant parameters on the average density changes at different cross sections downstream of the fire were the same as the significant parameters on the average temperature changes, as shown in Fig. 9b. Although the HRR had a significant influence on the average viscosity changes at the cross section 1 (20 m downstream of the fire), the effect of HRR on the changes of the average viscosity at the other cross sections (cross sections 2, 3, and 4) downstream of the fire was inconsequential as shown in Fig. 9c. Due to the high temperature close to the fire source in 30 MW scenarios compared to the scenarios with 10 MW fire, the HRR had a drastic impact on the average viscosity changes. At cross section 2 (120 m downstream of the fire source) and further downstream of the fire, the average viscosity was not changed significantly by changing the HRR from 10 MW to 30 MW as shown in Fig. 9c. The inlet air velocity was observed to be the only significant parameter effecting the average viscosity at all selected cross sections downstream of the fire. The reason lies in the upwind transport of the smoke (rollback) in the scenarios with the inlet air velocity less than critical velocity $V < V_{cr}$ (scenarios 3, 4, 5, and 8). Therefore, the average air viscosity downstream of the fire in these scenarios is lower compare to the scenarios with the inlet air velocity greater than equal to the critical velocity $V \geq V_{cr}$ (5 m/s) (scenarios 1, 2, 6, and 7). The significant

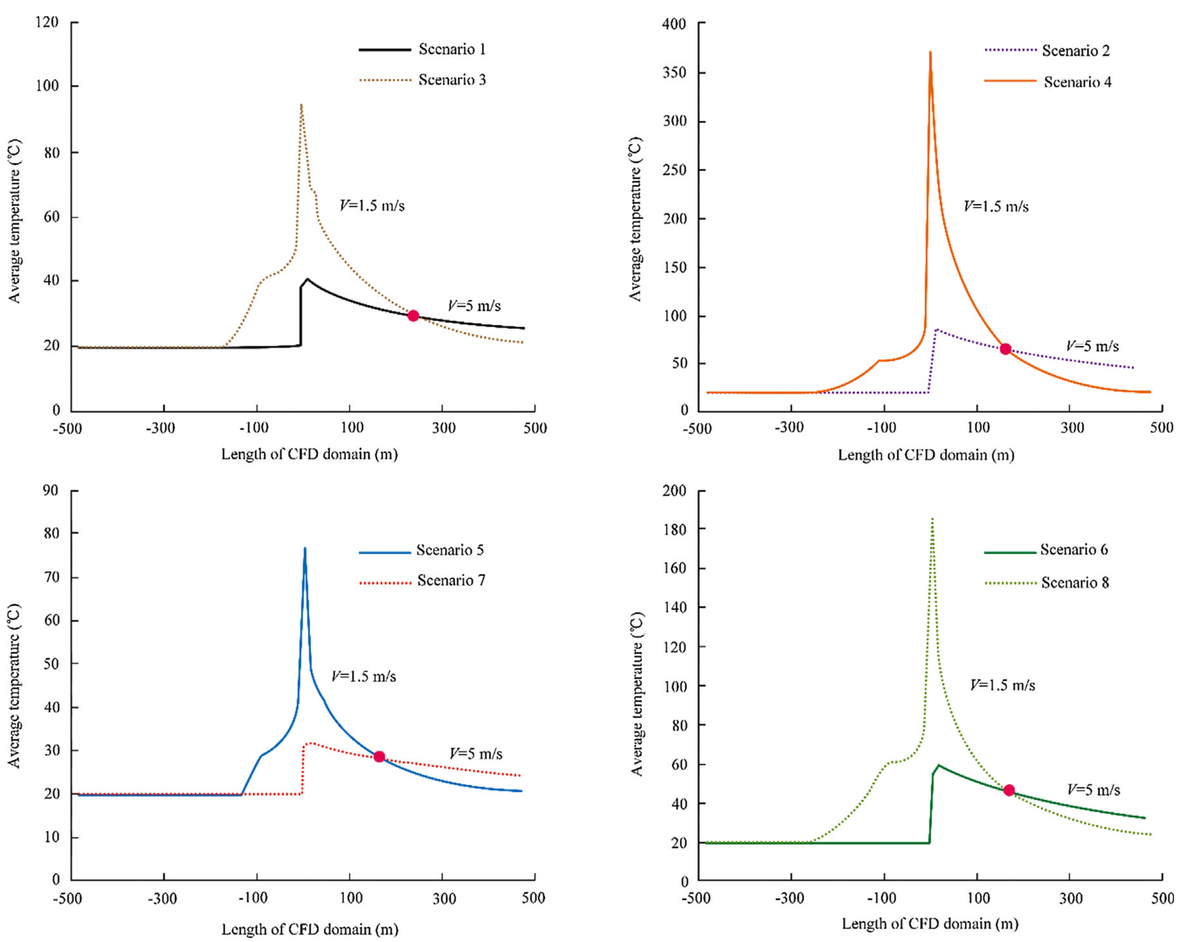

Fig. 10. Effect of the inlet air velocity on the average temperature along the height of the tunnel at different cross sections in different scenarios at $t = 900$ s.

parameters on the average velocity changes at all cross sections downstream of the fire were the inlet air velocity and the HRR as shown in Fig. 9d. Since the fixed flow was set at the tunnel inlet in all scenarios, the impact of tunnel cross section on the average velocity changes was insignificant. It is noteworthy that the physical size of the fire (fire perimeter) did not have the significant effect on the response variables at all cross sections downstream of the fire (from 20 m downstream of the fire to 400 m downstream of the fire).

Overall, by getting further away from the fire source, the domination of tunnel dimension on the changes of the average temperature and the average density downstream of the fire decreased. The changes of the tunnel dimension did not influence the average velocity and the average viscosity downstream of the fire (If the fixed flow were set at the inlet of the computational domain). The only two significant parameters on the changes of the average temperature, average density, and the average velocity 400 m downstream of the fire source, were HRR and the inlet velocity; and also the only significant parameter on the changes of the average viscosity, 400 m downstream of the fire was the inlet velocity. The fire perimeter was an insignificant parameter on the changes of the response variables at all cross sections downstream of the fire. It is noteworthy that the parameters interactive effects on the response variables (e.g., average temperature, the average density, the average velocity, and the average viscosity) at all cross sections downstream of the fire were also insignificant.

6. Conclusions

The significance of tunnel dimensions, inlet air velocity, heat release rate, and the physical fire size (fire perimeter) on the fluid characteristics downstream of the fire source were quantified using CFD simulations data from a test program that was conducted based on a statistical two-level design known as the fractional factorial design. Based on the prediction of the designed statistical models, the linear models were found to provide statistically good prediction. The effect of computational domain length on the selection of the significant parameters downstream of the fire source was analyzed. Based on the parametric evaluation, the key parameters effects and the parameters interactive effects on different response variables (e.g., average temperature, average density, average viscosity, and average velocity) at different cross section downstream of the fire were determined individually.

It is noteworthy that by getting further from the fire source, the number of significant parameters on the response variable changes downstream of the fire decreased. This study has shown that the changes of the physical size of the fire did not influence the average temperature, average velocity, average density, and average viscosity downstream of the fire source. In addition, it was observed that the interactive effect of the parameters was inconsequential on the changes of the average temperature, average density, average velocity, and the average viscosity downstream of the fire source. Therefore, these parameters don't have to be investigated in detail in any numerical analysis study on the aforementioned response variables for 10–30 MW fires in future tunnel fire studies. It is noteworthy that the HRR changes could change the average viscosity close to the fire source (20 m downstream of the fire). However, the effect of HRR on the average viscosity was inconsequential at 120 m downstream of the fire source and further. Due to effect of the velocity on the upstream transport of the smoke (e.g., scenarios with inlet air velocity less than critical velocity ($V < V_{cr}$)), the only key parameter on the average viscosity changes at all cross sections of the tunnel downstream of the fire was the inlet air velocity. Since the density is temperature dependent, the significant parameters on the average temperature and significant parameters on the average density were the same at all cross sections downstream of the fire. The tunnel dimension was one of the key parameters on the changes of the average temperature and the average density through 20–220 m downstream of the fire source; the tunnel dimension effect on the average temperature and the average density was insignificant 400 m downstream of the fire. In addition, the HRR was the only parameter which had significant impact on the average temperature and the average density at all cross sections downstream of the fire. Although the inlet velocity influenced the average temperature and the average density drastically at 20 m and 400 m downstream of the fire source (e.g., cross sections 1 and 4), an inconsequential impact of the inlet velocity on the average temperature and the average density was observed at 120 m and 220 m downstream of the fire (e.g., cross sections 2 and 3). In addition, it was evident that the average velocity at all cross sections downstream of the fire was affected significantly by the changes of the inlet velocity and the HRR. Therefore, the significant parameters on the average velocity changes at all cross sections downstream of the fire were selected as the inlet air velocity and the HRR.

The proposed statistical analysis was demonstrated to be a useful technique for screening the significant parameters on the fluid characteristics downstream of the fire source. Robust emergency response layout design and fire safety plan require numerous simulations to support evaluating the safety of the underground environment. Understanding and screening the key parameters on the fluid characteristics downstream of the fire is required for decreasing the number of fire simulations for future studies and for improving the tunnel fire safety plan of the occupants.

Acknowledgement

This research was developed under Contract No. 200-2014-59669, awarded by the National Institute for Occupational Safety and Health (NIOSH). The findings and conclusions in this work are those of the authors and do not reflect the official policies of the Department of Health and Human Services; nor does mention of trade names, commercial practices, or organizations imply endorsement by the U.S. Government.

Appendix A

The calculated values for the response variables at 20 m, 220 m, and 400 m downstream of the fire source (e.g., cross sections 1, 3, and 4) are provided in Tables A1, A2, and A3, respectively.

Table A1
Summary of independent parameters and measured values for the response variable at cross section 1 (20 m downstream of the fire source) at $t = 900$ s.

Scenario No.	Response variables			
	Temperature (°C)	Density (kg/m^3)	Velocity (m/s)	Viscosity (kg/(m·s))
Scenario 5	47.22	1.11	1.74	0.00434
Scenario 8	104.07	0.98	2.11	0.00539
Scenario 2	83.70	1.00	6.29	0.01107
Scenario 1	39.96	1.13	5.51	0.00981
Scenario 3	67.80	1.04	1.87	0.00409
Scenario 4	228.90	0.77	2.61	0.00548
Scenario 7	31.65	1.15	5.46	0.00891
Scenario 6	60.02	1.08	5.94	0.01167

TableA2
Summary of independent parameters and measured values for the response variable at cross section 3 (220 m downstream of the fire source) at t = 900 s.

Scenario No.	Response variables			
	Temperature (°C)	Density (kg/m^3)	Velocity (m/s)	Viscosity (kg/(m·s))
Scenario 5	25.16	1.17	1.63	0.00167
Scenario 8	38.42	1.13	1.82	0.00188
Scenario 2	61.16	1.05	5.89	0.00509
Scenario 1	30.75	1.15	5.31	0.00544
Scenario 3	31.66	1.15	1.71	0.00156
Scenario 4	50.70	1.09	1.93	0.00198
Scenario 7	27.09	1.17	5.30	0.00593
Scenario 6	42.38	1.11	5.59	0.00584

Table A3
Summary of independent parameters and measured values for the response variable at cross section 4 (400 m downstream of the fire source) at t = 900 s.

Scenario No.	Temperature (°C)	Density (kg/m^3)	Velocity (m/s)	Viscosity (kg/(m·s))
Scenario 5	21.30	1.19	1.62	0.00158
Scenario 8	26.63	1.17	1.78	0.00180
Scenario 2	46.71	1.10	5.75	0.00529
Scenario 1	26.72	1.17	5.28	0.00559
Scenario 3	22.89	1.19	1.69	0.00155
Scenario 4	24.76	1.18	1.88	0.00166
Scenario 7	24.91	1.18	5.28	0.00603
Scenario 6	34.82	1.14	5.51	0.00586

Appendix B

The probability of the significant parameters or significant associated interactions on various responses at 20 m, 220 m, and 400 m downstream of the fire source (e.g., cross sections 1, 3, and 4) are shown in Tables B1, B2, and B3, respectively.

Table B1
Statistical significance of the parameters and their associated interactions along with fit analysis for the models at cross section 1 (20 m downstream of the fire source).

Temperature		Viscosity		Velocity		Density	
Parameter	T-Statistic	Parameter	T-Statistic	Parameter	T-Statistic	Parameter	T-Statistic
Model	0.0003	Model	<0.0001	Model	<0.0001	Model	0.0077
B-HRR	<0.0001	A-Inlet air velocity	<0.0001	A-Inlet air velocity	<0.0001	B-HRR	0.0050
A-Inlet air velocity	0.0003	B-HRR	0.0032	B-HRR	0.0088	A-Inlet air velocity	0.0161
D-Tunnel dimension	0.0009	R-Squared	0.9863	R-Squared	0.9929	D-Tunnel dimension	0.0321
R-Squared	0.9978	Adj. R-Squared	0.9808	Adj. R-Squared	0.9901	R-Squared	0.9351
Adj. R-Squared	0.9950					Adj. R-Squared	0.8864

Table B2
Statistical significance of the parameters and their associated interactions along with fit analysis for the models at cross section 3 (220 m downstream of the fire source).

Temperature		Viscosity		Velocity		Density	
Parameter	T-Statistic	Parameter	T-Statistic	Parameter	T-Statistic	Parameter	T-Statistic
Model	0.0003	Model	<0.0001	Model	<0.0001	Model	0.0156
B-HRR	<0.0001	A-Inlet air velocity	<0.0001	A-Inlet air velocity	<0.0001	B-HRR	0.0044
D-Tunnel dimension	0.0016			B-HRR	0.0147	D-Tunnel dimension	0.0272
R-Squared	0.9879	R-Squared	0.9810	R-Squared	0.9992	R-Squared	0.9656
Adj. R-Squared	0.9788	Adj. R-Squared	0.9778	Adj. R-Squared	0.9981	Adj. R-Squared	0.9197

Table B3
Statistical significance of the parameters and their associated interactions along with fit analysis for the models at variable at cross section 4 (400 m downstream of the fire source).

Temperature		Viscosity		Velocity		Density	
Parameter	T-Statistic	Parameter	T-Statistic	Parameter	T-Statistic	Parameter	T-Statistic
Model	0.0019	Model	<0.0001	Model	<0.0001	Model	0.0355
A-Inlet air velocity	0.0031	A-Inlet air velocity	<0.0001	A-Inlet air velocity	<0.0001	A-Inlet air velocity	0.0299
B-HRR	0.0034			B-HRR	0.0135	B-HRR	0.0337
R-Squared	0.9181	R-Squared	0.9894	R-Squared	0.9994	R-Squared	0.9190
Adj. R-Squared	0.8853	Adj. R-Squared	0.9876	Adj. R-Squared	0.9987	Adj. R-Squared	0.8432

References

[1] Caliendo C, Ciambelli P, De Guglielmo ML, Meo MG, Russo P. Numerical simulation of different HGV fire scenarios in curved bi-directional road tunnels and safety evaluation. Tunn Undergr Space Technol 2012;31:33–50.

[2] Beard A, Carvel R. The handbook of tunnel fire safety, Part V, emergency procedures. London: Thomas Telford Ltd.; 2005. p. 536.

[3] Babrauskas V, Peacock RD. Heat release rate: the single most important variable in fire hazard. Fire Saf J 1992;18:255–72.

[4] Ingason H, Li YZ, Lönnermark A. Tunnel fire dynamics. New York: Springer Science+Business Media; 2015.

[5] Fan CG, Li YZ, Ingason H, Lonnermark A. Effect of tunnel cross section on gas temperatures and heat fluxes in case of large heat release rate. Appl Therm Eng 2016;93:405–15.

[6] Rickard H. Fire behavior of mining vehicles in underground hard rock mines. Int J Min Sci Technol 2017;27:627–34.

[7] Ingason H, Lönnermark A. Heat release rates from heavy goods vehicle trailer fires in tunnels. Fire Saf J 2005;40:646–68.

[8] Migoya E, García J, Crespo A, Gago C, Rubio A. Determination of the heat release rate inside operational road tunnels by comparison with CFD calculations. Tunn Undergr Space Technol 2011;26:211–22.

[9] Seike M, Kawabata N, Hasegawa M. Quantitative assessment method for road tunnel fire safety: development of an evacuation simulation method using CFD-derived smoke behavior. Saf Sci 2017;94:116–27.

[10] Owen M, Galea ER, Lawrence PJ. The exodus evacuation model applied to building evacuation scenarios. J Fire Prot Eng 1996;8(2):65–86.

[11] Galea ER, Galparsoro JMP. A computer based simulation model for the prediction of evacuation from mass transport vehicles. Fire Saf J 1994;22:341–66.

[12] Gwynne S, Galea ER, Lawrence PJ, Filippidis L. Modelling occupant interaction with "re conditions using the building EXODUS evacuation model. Fire Saf J 2001;36:327–57.

[13] McGrattan K, Hostikka S, McDermott R, Floyd J, Weinschenk C, Overholt K. Fire Dynamics Simulator Technical Reference Guide, vol. 1. Mathematical Model, 6th ed. USA: NIST Special Publication; 2014. p. 1018.

[14] Montgomery DC. Design and analysis of experiments. 8th ed. Canada: John Wiley & Sons, INC.; 2012.

[15] Mukerjee R, Wu CFJ. A modern theory of factorial designs. New York: Springer; 2006.

[16] Anderson MJ, Whitcomb PJ. DOE simplified: practical tools for effective experimentation. 3rd ed. India: CRC Press; 2015.

[17] Box GEP, Hunter WG, Hunter JS. Statistics for experimenters: an introduction to design, data analysis, and model building. Wiley series in probability and mathematical statistics. New York: John Wiley & Sons, Inc.; 1978.

[18] Morgado LV. Design of experiments applied to aerodynamic simulation of a sub-compact vehicle. In: Proceedings of SAE Brasil congress and exhibit; 2004. http://doi.org/10.4271/2004-01-3250.

[19] National Fire Protection Association (NFPA). NFPA® 502, Standard for Road Tunnels, Bridges, and Other Limited Access Highways. Quincy: National Fire Protection Association; 2011.

[20] Maidl B, Thewes M, Maidl U. Handbook of tunnel engineering II, basics and additional services for design and construction. Berlin: Ernst & Sohn GmbH & Co; 2014.

[21] Hung CJ, Monsees J, Munfah N, Wisniewski J. Technical Manual for Design and Construction of Road Tunnels-Civil Elements, Report No. FHWA-NHI-10-034. Washington, DC: Federal Highway Administration; 2009.

[22] Kim HK, Lönnermark A, Ingason H. Effective firefighting operations in road tunnels. Sweden: SP Technical Research Institute of Sweden; 2010.

[23] Schmidt FW, Henderson RE, Wolgemuth CH. Introduction to thermal sciences: thermodynamics, fluid dynamics, heat transfer. 2nd ed. New York: Wiley; 1984.

[24] Oka Y, Atkinson GT. Control of smoke flow in tunnel fires. Fire Saf J 1995;25:305–32.

[25] Wu Y, Bakar MZA. Control of smoke flow in tunnel fires using longitudinal ventilation systems-a study of the critical velocity. Fire Saf J 2000;35:363–90.

[26] Vauquelin O, Wu Y. Influence of tunnel width on longitudinal smoke control. Fire Saf J 2006;41:420–6.

[27] Kunsch JP. Simple model for control of fire gases in a ventilated tunnel. Fire Saf J 2002;37:67–81.

[28] Hwang CC, Edwards JC. The critical ventilation velocity in tunnel fires-a computer simulation. Fire Saf J 2005;40:213–44.

[29] Ingason H. Design fire curves for tunnels. Fire Saf J 2009;44:259–65.

[30] DiNenno P, Beyler C, Custer R, Walton W. SFPE handbook of fire protection engineering. 2nd ed. Quincy: National Fire Protection Association; 1995.

[31] Bamforth B, Chisholm D, Gibbs J, Harrison T. Properties of concrete for use in Eurocode 2: how to optimise the engineering properties of concrete in design to Eurocode 2. London: The Concrete Centre; 2008.

[32] Laage LW, Greuer RE, Pomroy WH. MFIRE users' manual. Version 2.20; 1995.

[33] Hassn A, Chiarelli A, Dawson A, Garcia A. Thermal properties of asphalt pavements under dry and wet conditions. Mater Des 2016;91:432–9.

[34] McGrattan K, Baum H, Rehm H. Large eddy simulation of smoke movement. Fire Saf J 1998;30:161–78.

[35] Baum HR, McCaffrey BJ. Fire induced flow field-theory and experiment. Fire Saf Sci 1989;2:129–48. https://doi.org/10.3801/IAFSS.FSS.2-129.

[36] Yuan L, Mainiero RJ, Rowland JH, Thomas RAT, Smith ACS. Numerical and experimental study on flame spread over conveyor belts in a large-scale tunnel. J Loss Prev Process Ind 2014;30:55–62.

[37] Deardorff JW. Stratocumulus-capped mixed layers derived from a three-dimensional model. Bound-Layer Meteorol 1980;18:495–527.

[38] Pope SB. Turbulent flows. British: Cambridge University Press; 2000.

[39] McGrattan K, Hostikka S, McDermott R, Floyd J, Weinschenk C, Overholt K. Fire dynamics simulator user's guide. 6th ed. USA: NIST Special Publication; 2014. p. 1019.

[40] Van Maele K, Merci B. Application of RANS and LES field simulations to predict the critical ventilation velocity in longitudinally ventilated horizontal tunnels. Fire Saf J 2008;43:598–609.

[41] Freedman D. Statistical models: theory and practice. Cambridge: Cambridge University Press; 2005.

[42] Freedman D, Pisani R, Purves R. Statistics. New York: W. W. Norton & Company; 1998.

[43] Lyman O, Longnecker M. An introduction to statistical methods and data analysis. 5th ed. California: Duxbury/Thomson Learning; 2001.